

Data Storage Report

SandT-Pro

Canal d'Invesitgació i Experimentació Marítima (CIEM), UPC



Authors: Joep van der Zanden, Dominic A. van der A
and Iván Cáceres

Status form

Document information

Project acronym	SandT-Pro
Provider	UPC
Facility	CIEM
Title	Measurements of Sand Transport and its underlying Processes under Large-Scale Breaking Waves
1st user group contact	Jan S. Ribberink, j.s.ribberink@utwente.nl
2nd user group contact	Dominic A. van der A, d.a.vandera@abdn.ac.uk
1st provider contact	Iván Cáceres, i.caceres@upc.edu
Start date experiment	04-11-2013
End date experiment	23-01-2014

Document history

Date	Status	Author	Reviewer	Approver
21-03-2014	Draft	Iván Cáceres		
04-04-2014	Draft	Joep van der Zanden Dominic van der A		
05-06-2014	Final	Joep, Dominic and Iván		

Document objective

This document describes the data that was obtained during this project and how it was stored, so that others than the people immediately involved may use the data for their research.

Acknowledgement

The work described in this publication was supported by the European Community's Seventh Framework Programme through the grant to the budget of the Integrating Activity HYDRALAB IV, Contract no. 261520.

Disclaimer

This document reflects only the authors' views and not those of the European Community. This work may rely on data from sources external to the HYDRALAB IV project Consortium. Members of the Consortium do not accept liability for loss or damage suffered by any third party as a result of errors or inaccuracies in such data. The information in this document is provided "as is" and no guarantee or warranty is given that the information is fit for any particular purpose. The user thereof uses the information at its sole risk and neither the European Community nor any member of the HYDRALAB IV Consortium is liable for any use that may be made of the information.

Contents

1 Objectives.....	4
2 Experimental setup.....	4
2.1 General description.....	4
2.2 Definition of the coordinate system.....	5
2.3 Relevant fixed parameters.....	5
2.3.1 Fixed parameters.....	5
3 Instrumentation and data acquisition.....	8
3.1 Instruments.....	8
3.2 Definition of time origin and instrument synchronization.....	21
4 Experimental procedure and test program.....	23
5 Organization of data files.....	34
6 References.....	36

1 Objectives

This report describes a series of test experiments carried out by Dominic Van der A, Joep van der Zanden, Sjoerd van Til, Quim Sospedra and Iván Cáceres in the CIEM wave flume. The experiments were done between 04 November 2013 and 23 January 2014, as part of the Hydralab IV access project “*Measurement of Sand Transport and its underlying Processes under Large-Scale Breaking Waves*” (SandTPro) and the EPSRC/STW funded project “*Sand transport under Irregular and Breaking Wave Conditions*” (SINBAD).

The main scientific objectives of the experiments in 2013/2014 are:

1. To improve understanding of the near-bed hydrodynamics and sand transport processes occurring under *large-scale* irregular non-breaking waves and regular breaking waves in the sheet flow regime by using new advanced high-resolution measuring instruments.
2. To improve understanding of how net suspended transport rates and total net transport rates can be related to overall flow and sediment parameters in a wide range of *large-scale* irregular non-breaking waves and regular breaking waves in the sheet flow regime.

The remainder of the report contains a description of the experimental set-up (Section 2); description of the used measurement instrumentation (Section 3); the experimental procedures and test conditions (Section 4), and the organization of the data files (Section 5).

The experiments with **regular breaking waves (RB)** will focus on research issues as i) the (timing of the) expected additional stirring caused by the breaking and how this affects the near-bed sediment fluxes and the wave-related flux in the suspension layer, ii) the flow non-uniformity and advection processes of turbulence and suspended sediment. Measurements under non-breaking waves in the same experiment and from previous large-scale experiments (Schretlen et al., 2010) will be used as reference.

The experiments with **irregular non-breaking waves (INB)** will focus on research issues as i) turbulence and sediment pumping under non-breaking irregular wave groups and how this affects the wave related sediment flux in the suspension layer ii) the effect of wave sequencing (within a wave group) on the near bed sediment flux and the flux above the wave boundary layer, and iii) which regular (non-breaking) wave (in terms of H and T) leads to the same net transport rate as a certain irregular (non-breaking) wave time-series (ie the equivalent wave concept).

The experiments will add substantially to existing knowledge of net sand transport rates and sand flux processes under breaking and irregular waves because of the large scale of the experiments (high Reynolds numbers and high sediment mobility numbers) and because of the high level of detail in the velocity and concentration measurements.

2 Experimental setup

2.1 General description

Experiments were conducted in the *Canal d'Invesitgació I Experimentació Marítima* (CIEM) wave flume at the Universitat Politècnica de Catalunya, (UPC), Barcelona. This large research facility is 100 m long, 3 m wide and 4.5 m deep (see Figure 1). The flume is fitted with a wedge type wave paddle with a maximum stroke of 2 m. There are five 0.9 m wide glass windows fitted at regular intervals along the flume test section and one large 5 m wide glass window near the onshore end of the flume allowing for visual observations and non-intrusive optical measurement techniques. The water depth at the wave paddle can be varied between 2.00m and 3.00m.

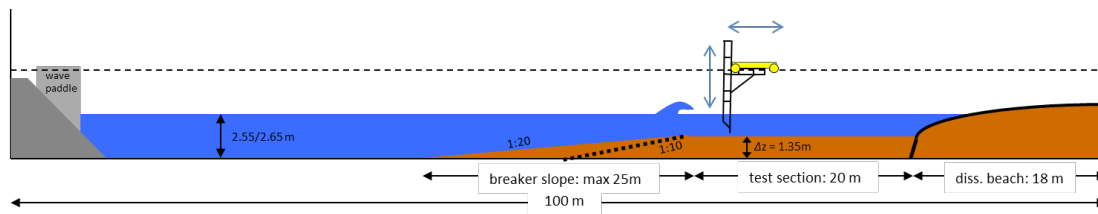


Figure 1. General set-up of the CIEM wave flume.

2.2 Definition of the coordinate system

The origin of the reference system used is placed in the middle of the stroke of the wave paddle and lies on the rigid bottom of the wave flume

- X follows the direction along the flume and is positive when going towards the shoreline. The absolute 0 is at the wave paddle in rest position, the profiles are referenced to that origin. The information about the instrumentation locations that can be found in this report refers to the marked guide in the flume which is 7.4 m from the wave paddle in the experimental clamping. This 7.4 m should be added to the instrumentation position in order to properly co-locate them in the flume.
- Z is directed vertically. The 0 is located at the upper part of the flume and is negative in downward direction until it reaches the value of -4.5 m at the bottom of the flume. Again when using this notation to report the instrumentation position it has to be mentioned that the information written in this report refers to the distance of the probe to the sandy bottom under it, this vertical coordinate is indicated with the small letter z.
- Y refers to the cross-shore distance of the flume. Only a few notations have been done using this reference and the 0 is at the wall in which the ADV's and Wave gauges were placed.

2.3 Relevant fixed parameters

2.3.1 Fixed parameters

The onshore end of the bed consisted of a fixed (non-mobile) parabolic shaped beach face with slope of about 1/15. The water depth at the toe of the wave paddle was fixed at about 2.55 m (RB1) and 2.65 m (INB1 and RB2) as presented in Table 4. For all conditions the paddle was clamped at the middle position of the hydraulic piston.

Sediment characteristics

The sediment used consisted of medium sand (d_{50} around 0.25 mm). The sand was provided by Sibelco and has the commercial name J5060S. The measured d_{50} of this sand sample is 246 μm (measured settling velocity of 34 mm/s).

Reference	50-60			
	Total Weight	199,192		
	Sieve (mm)	Weight	%	
	0,710	0,020	0,010%	0,010%
	0,595	0,027	0,014%	0,024%
	0,500	0,668	0,336%	0,360%
	0,350	26,006	13,093%	13,453%
	0,300	66,983	33,723%	47,175%
	0,210	54,242	27,308%	74,484%
	0,149	36,515	18,384%	92,867%
	0,125	13,070	6,580%	99,447%
	0,105	0,738	0,372%	99,819%
	0,088	0,240	0,121%	99,940%
	0,063	0,050	0,025%	99,965%
	Remainder	0,070	0,035%	100,000%
		198,629		

Table 1. Granulometry distribution for Sibelco J5060S.

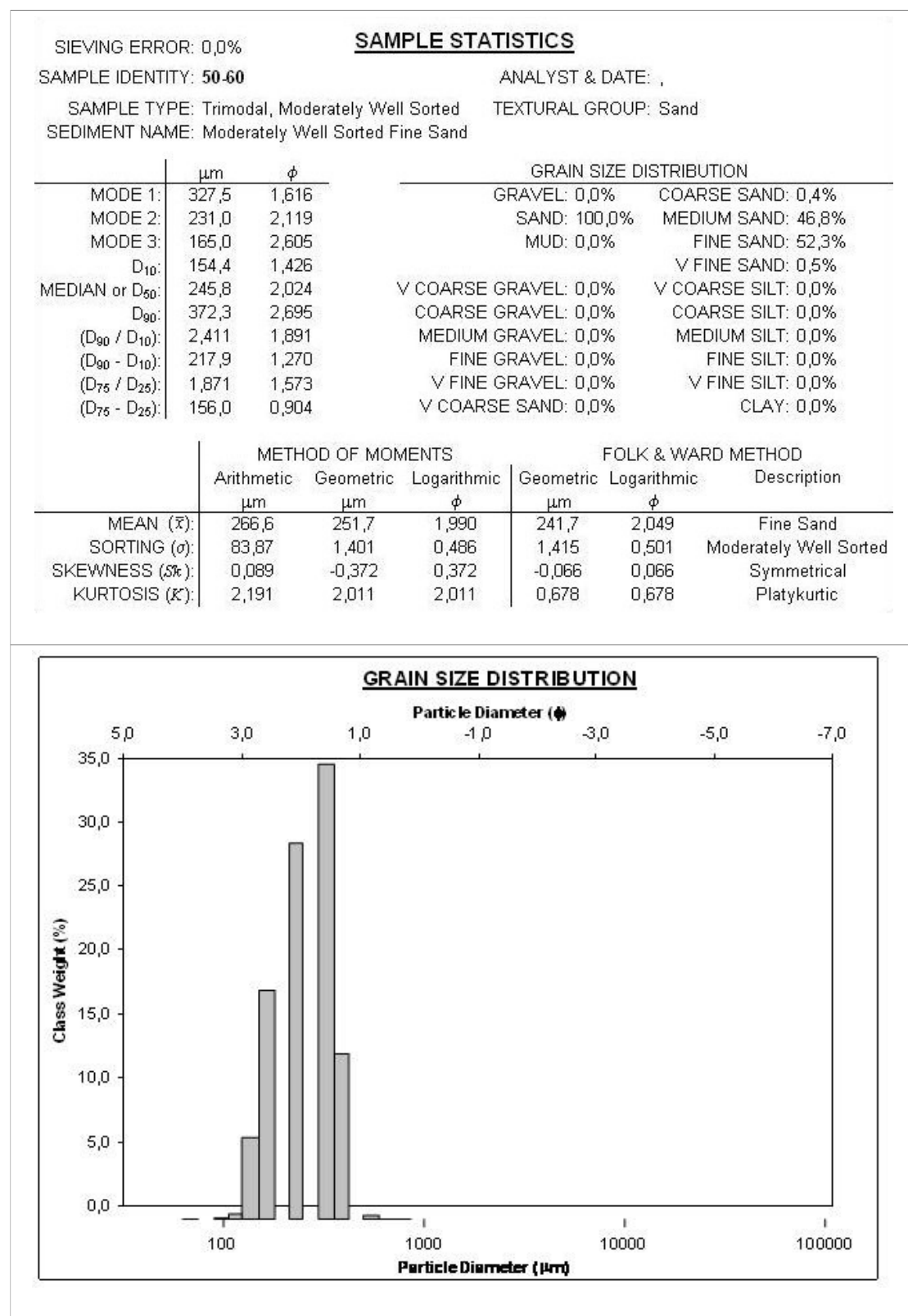


Figure 2. Grain size distribution for Sibelco J5060S.

3 Instrumentation and data acquisition

3.1 Instruments

The characteristics of the following instruments are described below:

1. Acoustic Doppler Velocimeter (ADV)
2. Vectrino Profiler
3. Acoustic Concentration and Velocity Profiler (ACVP)
4. Resistance Wave Gauges
5. Pressure Sensors
6. Bed Profiler
7. Optical Backscatter Sensor (OBS)
8. Acoustic Backscatter System (ABS)
9. Conductivity Concentration Meter (CCM)
10. Sand Ripple Profiler (SRP)
11. Transverse Suction System (TSS)

3.1.1 Acoustic Doppler Velocimeter (ADV)

Description

The Vectrino Velocimeter measures water speed using the Doppler effect. Provided by Nortek the Acoustic Doppler Velocimeter of the Vectrino type have the next characteristics:

The probe consist of four receive transducers, each mounted inside the receiver arm, and a transmit transducer in the center. The Vectrino uses the Doppler effect to measure current velocity by transmitting short pairs of sound pulses, listening to their echoes and, ultimately, measuring the change in pitch or frequency of the returned sound. Sound does not reflect from the water itself, but rather from particles suspended in the water (zooplankton or sediment). Every probe has a temperature sensor.

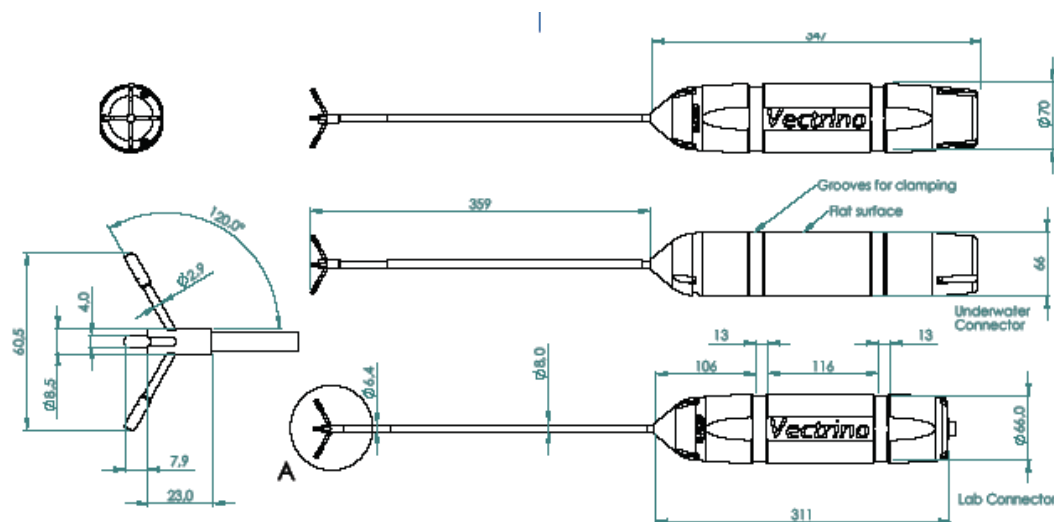


Figure 3. Nortek ADV vectrino sketch.

Calibration

To calibrate the probe there is a probe check feature within the Nortek software. This has been designed to act as a measurement quality assurance tool, by letting inspect the region where the Vectrino makes its measurements and showing how the signal varies with range.

Data acquisition

The data acquisition has been done by using the software (Polysinc), which allows the synchronization of the measuring ADV (up to 7) and the data synchronization of the acquired

information. The information is stored in .vno extension files that later on the program transform to several files (up to 6), from which the date, temperature, velocities, correlation of the signals, intensity of the signal ... can be easily recovered for every probe.

Specifications

Water Velocity Measurements

- Range $\pm 0.01, 0.1, 0.3, 1, 2, 4$ m/s*)
- Accuracy $\pm 0.5\%$ of measured value ± 1 mm/s
- Sampling rate (output) 1–25 Hz
- 1–200 Hz (Vectrino firmware)

Sampling Volume

- Distance from probe 0.05 m
- Diameter 6 mm
- Height (user selectable) 3–15 mm

Echo Intensity

- Acoustic frequency 10 MHz
- Resolution Linear scale
- Dynamic range 25 dB

Sensors

- Temperature Thermistor embedded in probe
 - Range -4°C to 40°C
 - Accuracy/Resolution $1^{\circ}\text{C} / 0.1^{\circ}\text{C}$
 - Time response 5 min

Power and data output

- DC Input 12–48 VDC
- Peak current 2.5 A at 12 VDC (user selectable)
- Max. consumption, 200 Hz 1.5 W
- Analog outputs 3 channels standard, one for each velocity component. Output range is 0–5 V, scaling is selectable.

Environmental

- Operating temperature: 5°C to 45°C
- Storage temperature: 15°C to 60°C

3.1.2 Vectrino Profiler

The Vectrino Profiler is a profiling Velocimeter that can measure the 3D velocity at rates up to 100 Hz. It is primarily designed for laboratory use but has successfully found use also in field applications such as swash velocity measurements on the beach. The basic measurement technology is coherent Doppler processing, which is characterized by accurate data at high rates with no appreciable zero offset.

The new Vectrino Profiler provides outstanding opportunities for high resolution observations of boundary layer dynamics and turbulence in the lab and the field. With the ability to profile three-component velocity (U,V,W) over a vertical range of 3 cm, with a resolution of 1 mm, and sampling rate of 100 Hz, the Vectrino Profiler allows new insight for a wide range of scientific studies.

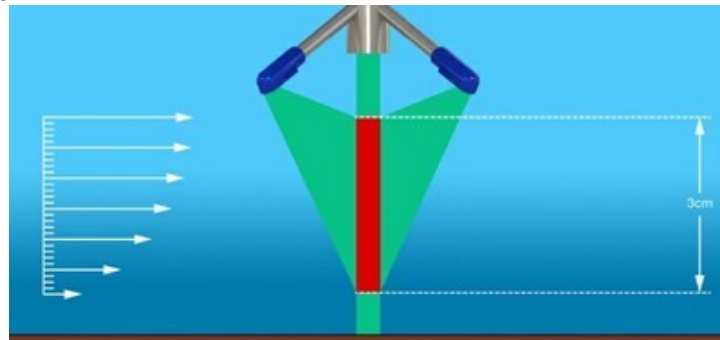


Figure 4. Vectrino profiler measurement range.

The Vectrino Profiler comes with completely new electronics, firmware, and software. For the firmware, adaptive pinging schemes have been added to minimize the effect of "weak spots" in the current profile. The new interface software provides enhanced capabilities such as real-time contour plots and energy spectra. The new firmware allows 10 Hz bottom distance measurements to be interleaved with the high resolution velocity profile. The simultaneous measurement of velocity and bottom position simplifies the data analyses by allowing all the velocity data points to be referenced to the bottom position.

The data were translated into Matlab *.mat files using the Nortek ADV 2 software.

3.1.3 HR-ACVP

The High Resolution - Acoustic Concentration and Velocity Profiler (HR-ACVP) is capable of co-located high-resolution profiling of the 2C/3C velocity and sediment concentration fields, thus providing direct measurement of the sediment flux. In recent years, the spatio-temporal resolution, velocity and concentration sediment measurements have been improved significantly due to its multi-frequency capabilities (Hurther et al. 2011, Thorne and Hurther 2014). Moreover, novel processing methods have been developed and tested to overcome the common measurement limitations associated with Doppler noise effects, velocity aliasing and acoustic attenuation effects across the bottom boundary layer region. Measurements under waves or currents conditions in the presence of active sediment layers (bedload or sheet flow layers) can be obtained with significant turbulence levels, strong acceleration and / or velocity asymmetries (Hurther and Thorne 2011, Chassagneux and Hurther 2014, Naqshband et al. 2014). When combined to the Acoustic Bed Interface Tracking (ABIT) method proposed by Hurther and Thorne (2011), this system provides high-rate estimations of both the bedload and the suspension loads.

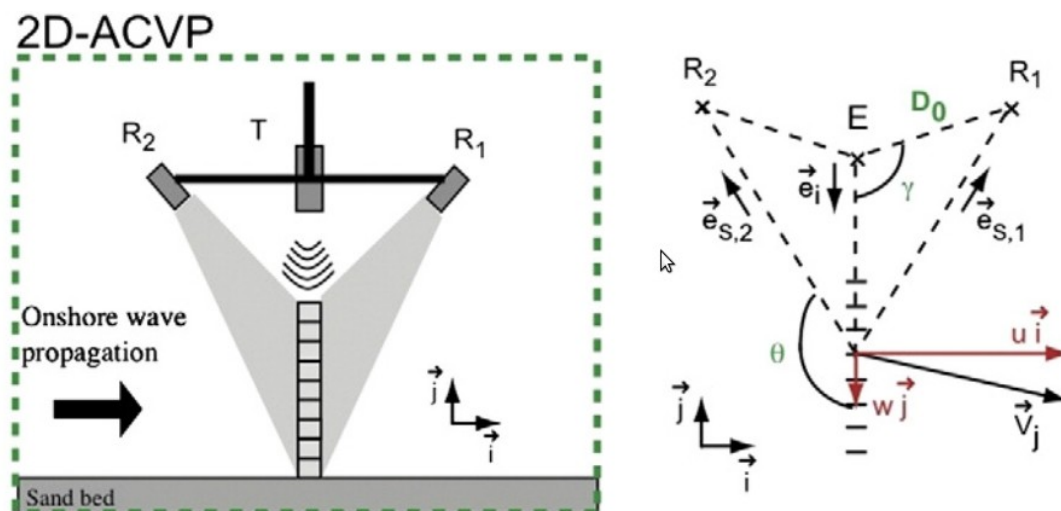


Figure 5. Configuration of the 2D-ACVP using one transceiver T (receiving mode is used for the concentration profiling) and 2 bi-static receivers R1 and R2 (Hurther et al. 2011)

3.1.4 Resistance Wave Gauges

Description

The resistance type wave gauges used in the CIEM operate on the principle of measuring the current flowing in an immersed probe which consists of a pair of parallel stainless steel wires (the absence of other support reduces the interaction between the measuring device and the incoming/reflected waves). The current flowing between the probe wires is proportional to the depth of immersion and this current is converted into an output voltage proportional to the instantaneous depth of immersion. The output circuitry is suitable for driving both a chart recorder and a data logger.



Figure 6. Resistive wave gauge.

Each wave probe needs a wave probe monitor with the energising and sensing circuits for the operation. Each monitor contains the circuits required to compensate for the resistance of the cable that is connected to the probe. Without this, the output of the wave probe monitor would be non-linear. In order to avoid polarization effects at the probe surface, a high frequency square wave voltage is used to energize the probe. The oscillator that produces this square wave may be set to one of six different frequencies. This allows probes to be used close together without causing any interference.

The current in each probe is detected by measuring the voltage drop across two resistors. Because the measured voltage is alternating, the signal is fed to a precision rectifier to produce a DC voltage proportional to the wave height. This signal feeds a small centre-zero balance indicator and a BNC socket on the front of the panel. The signal is also fed to a preset gain stage that may be set for a gain of between 0.5 and 10. Controls on the front of each wave probe module enable the output signal to be set to zero for any given initial depth of probe immersion. This, together with the gain adjustment, produces a full-scale output of $\pm 10V$ for all waves.

Application range

The steel wires' length allows detecting any wave height up to 2m.

Calibration

The transformation function (from voltage to depth) is calibrated due the possible changes in the water conductivity (temperature and salinity concentration effects). An overall calibration from wave height to output voltage can be performed by measuring the change in output voltage, while raising or lowering the mean water level of the flume.

Data acquisitions

Voltages from the resistive wave gauges are captured on the laboratories' general data acquisition system. The data acquisition system supports the following hardware manufacturers:

- Data Translations boards which is supported by the Open-Layer interface.

- National Instruments boards supported by NI-DAQmx 8.6

The system supports data acquisition on several boards at the same time as long as they are from the same manufacturer. The system supports controlling of external equipment through digital and analog outputs which can be triggered on a specified time or by an input channel.

The system supports high throughput using hardware trigger which leads to little cpu utilization for even high sampling frequencies (>1 kHz).

Specifications

Output Signals: front of monitors $\pm 10V$ via BNC socket
 rear of case $\pm 10V$ via 25 way D socket
 Gain 0.5, 0.75, 1.0, 1.5, 2.55, 3.75, 6.0, 10.0
 Excitation frequency 4.6 kHz to 11.6 kHz
 Filter band width -3dB at 20Hz
 Supply voltage 220 or 110V $\pm 10\%$ 40-60Hz
 Active length 2000 mm
 Diameter 1.5 mm

3.1.5 Pore Pressure Sensors (PPT)



Figure 7. Pore Pressure Transducer

Description

Provided by STS the ATM/N pressure sensors have the next characteristics

Application range

Up to 100 or 400 mb (1 and 4 m of water respectively)

Calibration

They are calibrated by using a calibrated pipe.

Data acquisitions

The signal intensity output is related, taking into account the calibration curve of each probe, to water height.

Specifications

Accuracy	< 0.5		
Thermal shift	Zero	0.....70°C	0.06
		-25...85°C	0.08
Span		0.....70°C	0.015
		-25...85°C	0.02

3.1.6 Bed Profiler

Description

This is a mechanical profiler, made up of a mobile platform holding an arm with a wheel at its end. The platform moves with constant velocity through the flume, while the articulate arm changes the position adapting to the depth forms. A computer controls its movement and depth changes, acquiring the profile information.

The principal profile characteristics are summarized in next figure.

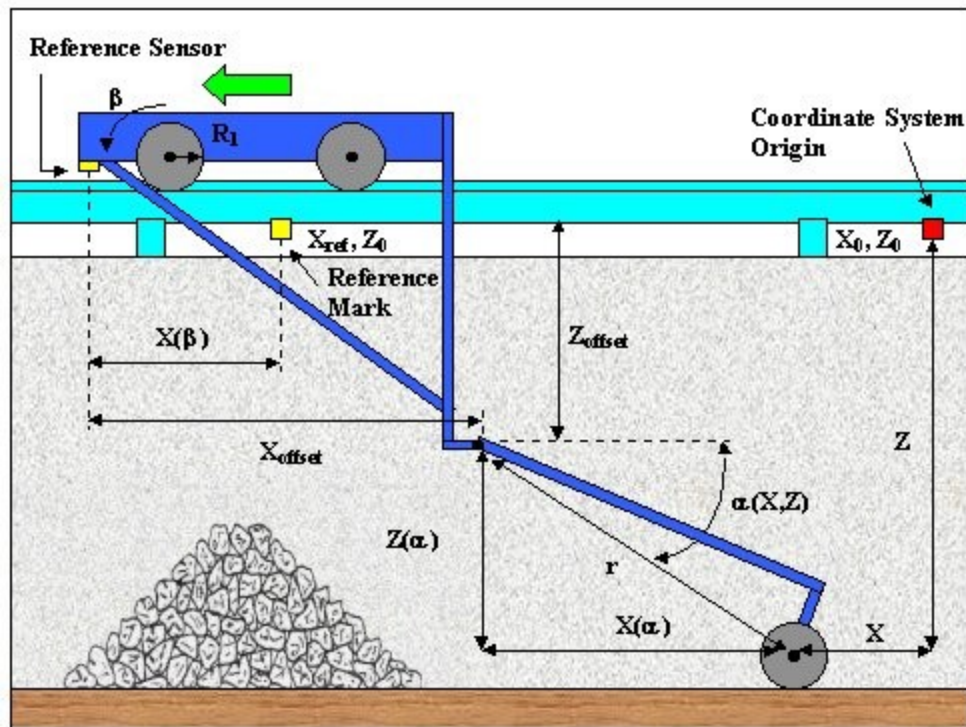


Figure 8. Sketch of mechanical profiler.

Arm length	3.00m
Wheel diameter	0.20m
r	3.15m
Z _{offset}	3.00m

Application range

The CIEM Profiler can be used to measure the emerged and submerged parts of beach profiles and was designed to be applied with arm angles (relative to horizontal plane) range from 0° to 50°. This means a maximum vertical range of 2.5m between the higher and lower beach profile points.

Calibration

The calibration is done by measuring different control points of known positions.

Data acquisitions

By controlling the carriage velocity and the angularity of the measuring arm the computer returns the profile signal as a system of X and Z coordinate along the flume dimensions. The arm angularity can be measured by means of an encoder or an inclinometer both located in the upper part of the arm.

Echosounders

Besides the mechanical wheel acquisition system there are also two echo sounder probes attached to the carriage. The echo sounder probes are UltraLab UWS with an ultrasound

sensor that operates at 1 MHz. These probes measure the profile evolution along the trolley position and this profile must be post-referenced to the bottom of the profile which is known and fixed. The measurements must always end on the fixed concrete floor of the flume. Note that in the present study the mechanical wheel profiler was not used, only the echosounders.

3.1.7 Optical Backscatter Sensor (OBS)

Description

The OBS sensor measures suspended solids and turbidity by the optical backscatter method. It features a compact micro probe that responds almost linearly over a 1000-fold change in sediment concentration and turbidity. These devices are supplied by D&A Instrument Company. The OBS-3+ model used in CIEM have the next characteristics:



Figure 9. Optical Backscatter Sensor

Application range

Ranges

Turbidity 0–2,000 NTU

Concentration Mud 0–2,500 mg/l

Sand 0–50 g/l

Accuracy

Turbidity 0.25 NTU or 1% of reading

Concentration Mud 0.5 mg/l or 1% of reading

Sand 0.25 g/l or 1% of reading

Calibration

The data calibration is specific of the kind of sediment, concentrations to be measured and water characteristics. The calibration is done following Butt et al. (2002), using glycerol, a clear fluid with higher viscosity than water which decreases the settling velocity and improves the signal reliability. During the calibration different known sand concentrations are introduced inside the control volume while recording the signal data. The sand and glycerol volume when performing the calibration must be as well mixed as possible.

Data acquisitions

The signal intensity output is related, taking into account the calibration table, to sediment concentration measurements.

Specifications

Voltage outputs	0–1.25 V, 0–2.50 V
Current output	4–20 mA
Maximum data rate	10 Hz
Infrared wavelength	850 nm
Maximum depth	500 m
Drift	< 2% / year
Power	5 V / 10 mA
Housing material	316 stainless steel or titanium
Dimensions	138 x 25 mm
Daylight rejection	–28 dB (re: 48 mW cm ^{–1})
Connector	MCBH-5-FS, wet-pluggable

3.1.8 Acoustic Backscatter Sensor (ABS)

The ABS instrument used is an AQUAScat 1000L from the Aquatec GROUP. The original system owned by UPC comes with three probes but the acquisition box has an extra input channel allowing a fourth transducer operating at a different frequency. Four transducers with a ceramic disc of 20 mm were used within this experiment with frequencies of 1, 2, 3 and 4 MHz frequencies (the 3MHz probe was supplied by National Oceanography Centre Liverpool). The acquisition frequency ranges between 1 and 64 Hz. The number of measured cells is up to 256 with a default bin size ranging between 10 to 40 mm (note that during the present experiments the software was unlocked to have bin size of 5 mm). The sediment range measurements typically go from 20 micrometers up to 2 mm and from 0.1 g/l up to 20 g/l over 1 m (these values depends on the measuring range). The cable distance between the transducers and the housing is 10 m.

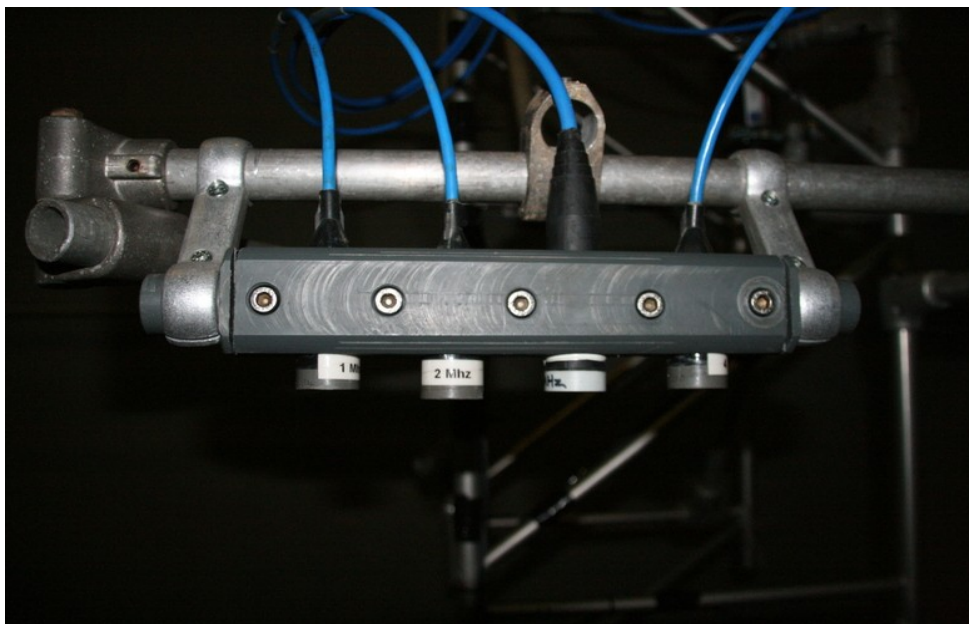


Figure 10. Acoustic Backscatter Sensor.

3.1.9 Conductivity Concentration Meter (CCM)

Figure 11 shows the two CCM tanks. The exterior of each tank is formed by a stainless-steel cylinder, closed at the top, and at the bottom welded to a steel base plate. The base plates can be mounted on the flume bottom or a palette, which in combination with the heavy weights (70 and 50 kg) of the tanks ensures the stability required to compensate for buoyancy and other destabilising effects.

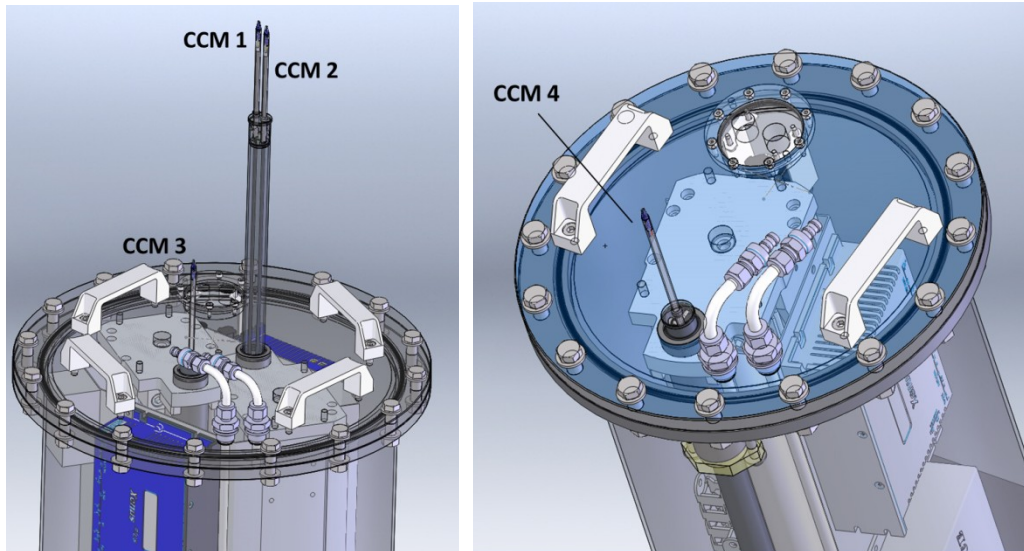


Figure 11. SolidWorks images of CCM Tanks. Left figure: tank 1 with CCM sensors 1 to 3; right figure: tank 2 with sensor 4.

The measuring probes are mounted to slim stainless-steel rods that emerge from the tanks. These rods can move vertically over a range of 28 cm. Each rod's position, and thus the position of the probes, is controlled with sub-mm accuracy by an electromagnetic servomotor in the corresponding tank. The rods leave the tanks through O-rings that prevent water and sand intrusion. The main difference between both tanks is the number of vertical rods and the number of measuring probes. The larger tank 1 contains three probes. Probes 1 and 2 are mounted to the same steel rod, and we will subsequently refer to this combined probe as 'probe 1/2'. Hence, tank 1 contains two servo-motors that control the positions of probe 1/2 and probe 3. Tank 2 contains one single probe and one motor. This sums up to a total of four probes (numbering is included in Figure 11). In order to accommodate both motors, tank 1 has a larger diameter than tank 2 (0.48 m and 0.38 m, respectively). Both tanks are 0.63 m high.

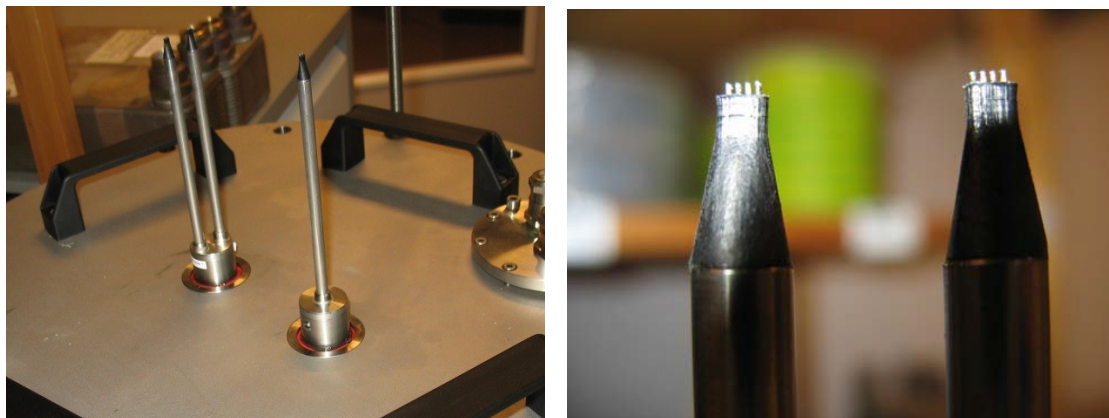


Figure 12. Snapshots of measuring probes tank 1 with rods in lowest position (left) and probe sensors (right).

Figure 12 shows how the probes are mounted to the vertical rods. The sensors in the top of each probe are formed by four platinum electrodes with a thickness of 0.3 mm and spacing of 0.6 mm (centre-to-centre), covered by an epoxy topping such that the exposed part of the electrodes is 0.8 mm high. The measuring principle of the sensors is conductivity-based, and relies on the linear relationship between sediment volume concentration C (m^3/m^3) and the

measured electrical conductivity of a sediment-water mixture U_m (V). Expressed in terms of voltages, this relationship reads as follows:

$$C = \left(1 - \frac{U_0}{U_m}\right) \cdot f_{cal} \quad (1)$$

where U_0 is the reference voltage for clear water (V), and f_{cal} is a dimensionless calibration factor that is usually close to 1. The reference voltage and calibration factor depend on local conditions and may drift slightly over time, as the probe is sensitive to both water temperature and the presence of ions. Before the start of any measurement, the voltages in clear water and in a loosely packed sand bed must be measured in order to obtain the proper values for U_0 and f_{cal} . When measuring, an alternating current is generated over the outer two electrodes while the inner two electrodes measure the electrical resistance of the water which is translated to a voltage U_m . Calibration graphs indicate that the measuring volume of the probes is 1 to 2 mm.

The sensors on probe 1/2 (tank 1) are aligned in the flow direction with a spacing of 1.5 cm, and can be used to determine sediment velocities through cross-correlation. The spacing between the two rods emerging from tank 1 is 9 cm (c.t.c.), normal to the direction of flow when the tanks are in use. Each tank is equipped with an optical sensor for leakage detection. In case of leakage, the control system automatically activates a peristaltic pump that is connected through a tube to the valves that are shown in Figure 11. Silica gel packages prevent condensation on the electronic devices inside the tanks. When applied, both tanks and rods are buried below the sand bed and only the probe sensors reach into the sheet-flow layer.

Within the CCM system, two types of signals are sampled: firstly, the measured voltage signals of the four CCM sensors, and secondly, the vertical positions of the three probes. The sampling frequency was 1000 Hz. The system is equipped with a new 'tracking system' that translates measured concentrations back into vertical sensor movement, such that the measuring sensors follow a certain target concentration. Hence one can choose to use a probe to follow bed-level changes rather than measuring sheet-flow layer concentrations. In this experiment we had the single probe (probe 3) of the larger tank following the bed, while the other probes were measuring concentrations at various sheet-flow layer elevations.

3.1.10 Sand Ripple Profiler (SRP)

Measurements of the local bed morphology were made with the Sand Ripple Profiler (see Figure 13). The SRP consists of a 2MHz disc transducer mounted on stepper motor, which are assembled in a waterproof aluminium and PVC housing. The transducer has a narrow conical beam pattern of 1.1° and the motor has a step size of 0.9° and can rotate radially over a 180° range. At each step of the stepper motor the SRP measures the acoustic backscatter over a profile consisting of 1000 samples, the total range of this profile can be adjusted over a 600mm to 6m range. The transducer is connected via a waterproof cable to the Electronics Processing Unit (EPU), which contains the transmitter/receiver electronics and the micro-controller. The EPU is connected via a serial RS232 cable to a PC, which controls the SRP through the supplied software package.



Figure 13: Sand Ripple Profiler

Calibration

No separate calibration is required for the SRP, but all distance calculations in the software are referenced to a fixed velocity of sound in water of 1500 m/s, therefore during post-processing of the SRP data the distances were corrected using the sound velocity from McKenzie (1981) based on the water temperature measured by the Vectrino Profiler.

Prior to the experiments a bed profile was made of the flume floor, see Figure 14 below. Although care was taken to mount the SRP transducer head with its zero marker directed vertically downward, the scan of the horizontal flume floor in Fig. 14(a) showed that the transducer head was in fact mounted under a slight angle (or the transducer disc is not perfectly aligned in the PVC housing). This angle of 4.90° was applied as an offset to all subsequent bed profiles (see Fig. 14(b)). At the end of the RB1 experiment the angle offset was again determined from a measurement of the horizontal flume floor, resulting in an angle of 4.86° , indicating practically no change in the transducer's position over the course of the RB1 experiment.

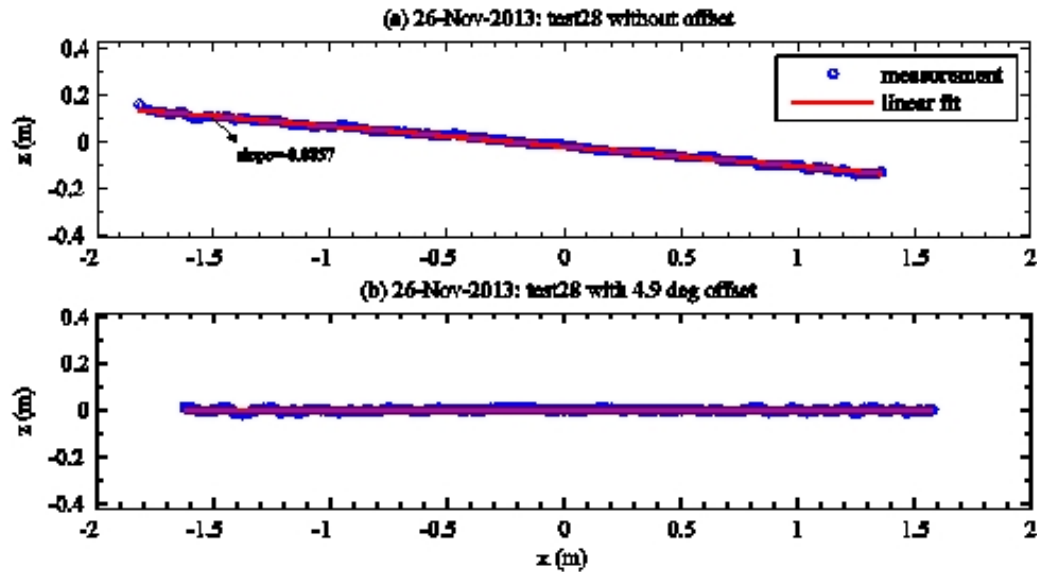


Figure 14. SRP measurement of the horizontal flume floor at $X=15.39\text{m}$ (corresponding to $x=0$); (a) without any angle offset showing that the transducer is mounted to the mobile frame at an angle of -4.90° , (b) corrected with an offset angle of 4.90 degree.

Data acquisition

For the present experiment, the SRP typically measured a profile in cross-shore direction of approximately $1.5\sim 2.0\text{m}$ in length, consisting of 135 bed measurements. For each experiment the bed was measured before the waves were started and after the waves were stopped. For selected runs the SRP was also scanning continuously during the experiment, resulting in a bed profile every 20-40s depending on the instrument's settings. It was not possible to do continuous profile measurements during every test since the SRP caused acoustic interference with the ABS signal, despite both instruments being located on opposite sides of the mobile frame. For this reason the ABS was always switched off during runs when the SRP was scanning continuously.

Specifications

The backscatter data produced by the SRP was post-processed using a bed recognition algorithm to yield the bed profile information. This algorithm essentially finds the peak in the bed echo by finding the level where the product of the backscatter and the gradient of the backscatter is maximum. This method was also used by O'Hara Murray et al. (2011). For the present experiment the along-beam resolution was typically 0.6mm or 1.2mm , but in practice the vertical accuracy is generally lower and reduces for decreasing grazing angles (i.e. at the edges of the profile). No separate validation tests were done (yet) to determine the accuracy, but previous studies have reported vertical accuracies of $\sim 5\text{mm}$ and within 10mm (Thorne et al., 2002; Doucette and O'Donoghue, 2006).

3.1.11 TSS and grain-size analysis

The Transverse Suction System (TSS) is an inexpensive method to measure time-averaged sediment concentrations. A TSS system (Figure 15) typically consists of several stainless steel intake tubes, flexible tubing and peristaltic pumps, which are a type of positive displacement pumps that can pump liquid solid mixtures in both directions. During the SandT-Pro experiment 7 nozzles were used connected through small tubes to 7 peristaltic pumps that were placed on the measuring trolley. Bosman et al. (1987) showed that the technique was applicable to waves, provided that direction of intake is normal to that of the ambient flow, and that the intake velocity exceeds the ambient flow velocity by a factor of

three at least. Satisfying these conditions ensures that the measurement is insensitive to flow direction, velocity magnitude and sediment size.

While for Bosman et al.'s (1987) small-scale wave flume experiments it was easy to obtain the required velocity ratio beyond three (their intake velocity was 1.3 m/s), they acknowledged that under full-scale wave conditions it would be difficult to achieve an intake velocity which is three times larger than the maximum orbital velocity. However, since maximum velocity only occurs for a relative short duration of the wave cycle they argued that it would only lead to a small systematic error (5% in case the intake velocity is only twice the maximum velocity) which was negligible to the random concentration error caused by other aspects of the design. Bosman et al. (1987) therefore expected that the requirement for the TS-method to have the velocity ratio (under waves) always beyond three was not very strict. Transverse suction systems based on Bosman et al.'s (1987) design recommendations have been successfully applied in full-scale experiments in oscillatory flow tunnels (LOWT, AOFT) and in wave flumes (GWK, Delta Flume).

For the RB1 series, pumps were started after the passing of about 5 waves. For the INB and RB2 series, runs were longer and the suction system was started after 5 minutes. The duration of suction varied between each run, but generally lasted until about 15 L of water was obtained. The volume of water was obtained by weighting the water + sediment sample. Subsequently, the samples were analysed using a sediment volume meter, which results in a volume of the wet sediment sample. By multiplying with $[1 - \text{porosity}] (=0.36)$ and the sediment density (1600 g/L), the dry mass of the sediment is obtained. The dry mass was multiplied with the calibration factor β to obtain the true concentration. For the INB runs, where little sediment was in suspension, samples were dried in an oven and weighted. For a few runs, samples were analysed with both the volume meter and by dry-weighing them, which yielded similar results.

The TSS system for the Barcelona wave flume facility required special design since the peristaltic pumps needed to be able to overcome a ~4m elevation head, i.e. the distance from the water surface to the top of the flume where the peristaltic pumps are located, while still maintaining a sufficiently large flow rate. Since the peristaltic pumps present in the research group (those used in previous AOFT TSS measurements) did not have sufficient capability all pumps were acquired by loan from other institutes. The tubing also needed careful consideration since in order to ensure a sufficiently large flow velocity the diameter needs to be kept small (and also to minimize flow disturbance by the tubing), while at the same time it needed to have large diameter to minimize the friction losses (and hence the output flow rate). Therefore, for each nozzle the submerged section of tubing consisted of 4mm ID (inner diameter) PE (Poly-Ethylene) flexible tubing, while above the water level the tubing consisted of 8mm ID PE tubing (this size still ensured flow velocities in the tube which were an order of magnitude larger than the settling velocity of sand). The pump discharge varied per nozzle/pump combination and per run, but was on average close to 1 L/min. This corresponds to an intake velocity of 2.4 m/s, which is approximately two times the maximum orbital velocity measured under the present wave conditions and therefore satisfies Bosman et al.'s design requirement. Table 2 presents an overview of the pump specifications of each nozzle.

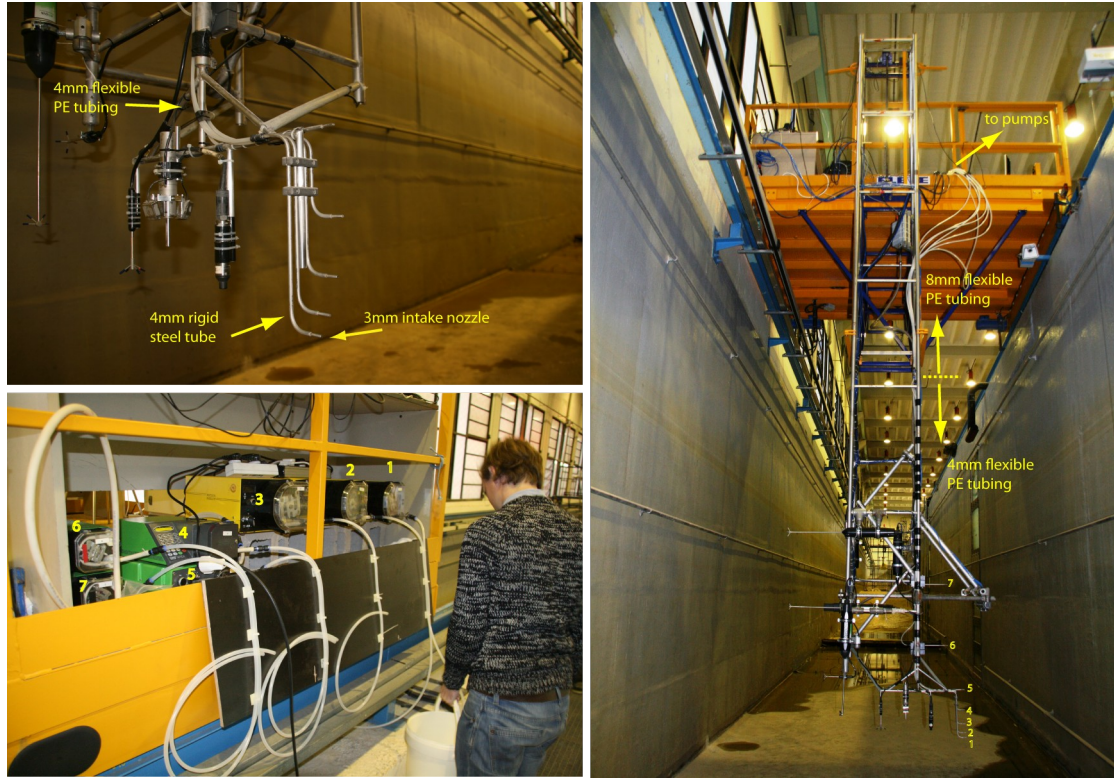


Figure 15. top left: close-up of intake nozzles on mini-frame; right: mobile frame showing all seven nozzle positions; bottom right: corresponding seven peristaltic pumps.

Nozzle	Pump	On loan from.
1	Watson Marlow 603S	FZK Hannover
2	Watson Marlow 603S	FZK Hannover
3	Watson Marlow 603S	FZK Hannover
4	Watson Marlow 505Di	Watson Marlow UK
5	Watson Marlow 504S	Marine Science Scotland
6	Watson Marlow 503S	Marine Science Scotland
7	Watson Marlow 503S	Marine Science Scotland

Table 2: TSS pump specifications

All suction samples were dried, stored in plastic bags, and transported to Aberdeen. There, the grain-size distribution of the contained samples was analysed. In addition, samples of the bed (at 8 positions) were taken after both breaking-wave conditions (RB1 and RB2).

The grain size measurements were conducted with a Beckman Coulter LS 13 320 in Aberdeen. This machine uses the diffraction of a laser to measure the grain sizes. After this analysis, the samples had to be discarded.

3.2 Definition of time origin and instrument synchronization

Most measuring equipment was synchronized by means of a TTL trigger signal. This signal has the origin on the General acquisition system of the CIEM flume. The signal starts with a 0 V and rises up to 5 V at the moment of starting the wave generation. For 1 second the time signal is at 5 V and later drops again to 0 V (as presented in Figure 16). The signal was sent to all the acquisition systems and each instrument started measuring on the rising edge of the signal or 1 second later on the falling edge of the signal (except the SRP and the CCM tank). Following the same notation as in the last section of this document (Organization of data files) the different data files are here listed depending on their time measurement starting point. The equipment that started on the rising edge of the trigger signal were: the general acquisition system (1_1), the ADV (1_3), and extra equipment (1_5). While the Aquascap (1_4), ACVP

(1_7) and ADV2 (1_9) started one second later to record on the falling edge of the trigger signal. Note that continuous SRP measurements were manually started within a few seconds of the trigger signal. The CCM (1_8) was started before the trigger signal was sent, and recorded the trigger voltage during the complete measurement. Due to trigger issues with the ADV2 (Vectrino Profiler), a separate trigger connection from the CCM system to the ADV2 was established for the RB2 runs. This continuous output trigger signal from CCM to ADV2 was stored in the CCM files. In runs where multiple output triggers were given from CCM to ADV2, the falling edge of the last trigger signal given by CCM should be used as the start of the ADV 2.

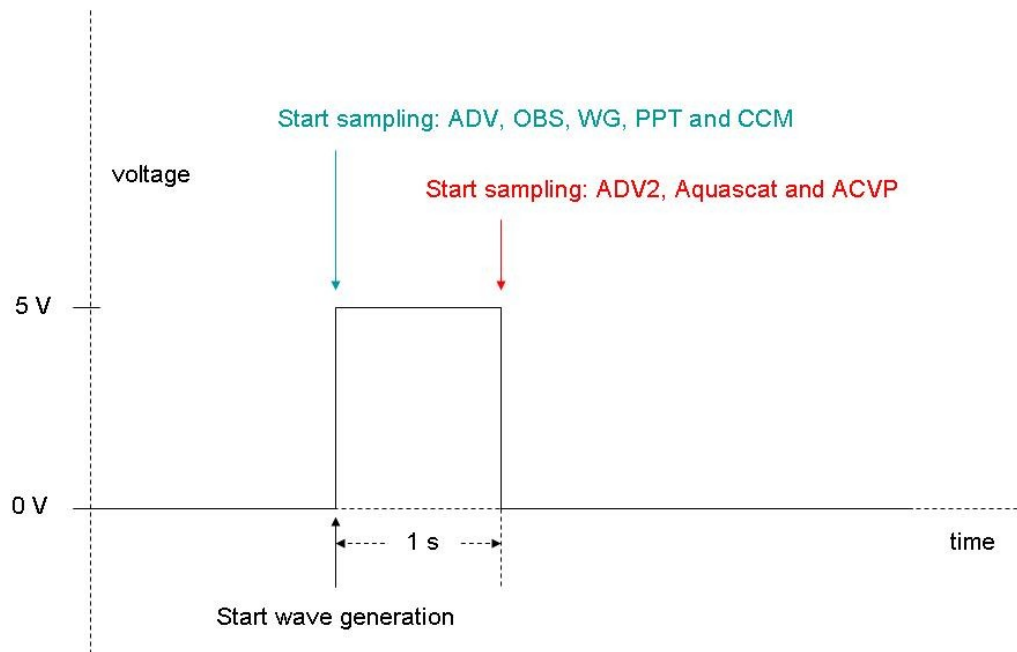


Figure 16. Trigger scheme.

The acquisition frequency of the general acquisition system (1_1_General_Acquisition) is 40 Hz. The OBS and PPT on the mobile frame (1_5_extra_equipment) have been acquired with a National Instrument external acquisition system at 100 Hz, but later on the information has been included in the Matlab binary files and converted to the 40 Hz similar to the general acquisition system.

The ADV's (1_3_ADV) have been measuring at 100 Hz with a transmit length of 0.6 mm and a sampling volume of 2.8 mm (all these parameters are standard for all the ADV). They were synchronized by means of two different computers pc1 for ADV 0 and 1 (fixed frame) while pc2 was controlling the ADV's on the mobile frame (ADV 2, 3, 4 and 5).

Acquisitions frequencies of the other measuring equipment.

- ADV2: 100 Hz, 30 vertical bins of 1 mm.
- ACVP: 36.7 Hz, 150 vertical bins of approximately 1.5 mm.
- CCM: 1000 Hz.
- ABS AquaScat: 64 Hz, 256 vertical bins of 5 mm. Measurement length of 1.28 m

For each run SRP bed levels were measured before and after wave action. During selected condition the bed levels were measured continuously during an experimental run, during these runs a bed profile was measured every 20-40s depending on the instrument's settings.

4 Experimental procedure and test program

During this set of experiments two different kind of equipment frames were deployed. Two fixed frames were mounted along the permanent aluminium bars of the flume during most of the experiment, therefore having a fixed cross- and longshore position. These frames had the same X cross-shore position and were only occasionally moved only in vertical direction during the experiments, the new location was noted in the daily report at the end of this section. The other equipment was mounted to the mobile frame (Figure 17). This mobile frame was able to move in two directions, along the flume's cross-shore direction (changing the X cross-shore location) and the vertical Z-position (changing the absolute Z distance towards the bottom of the flume). The mobile frame was relocated at the end of most of the tests. Due to this frequent movement, the X and Z location of the movable frame is noted in the 6th column of the experiment Table 3. The relative location of each instrument relative to the movable frame can be obtained from Figure 17 and table 3 (extract from logbook)

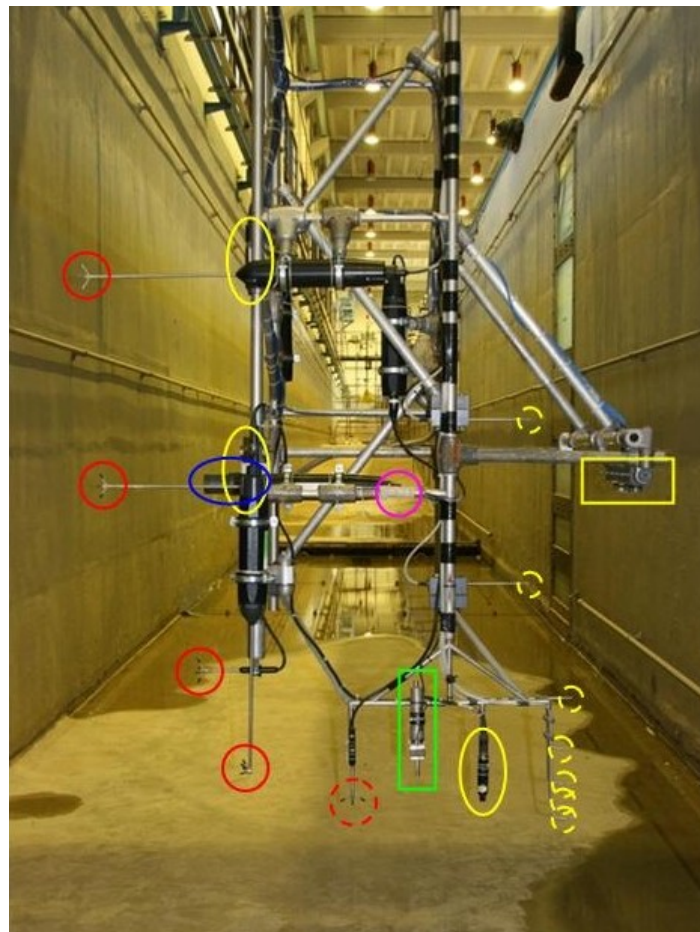


Figure 17. Mobile frame used during the SandT-Pro experiments. This mobile frame contained 4 ADV's (red circles), 1 Vectrino Profiler (red dashed circle), 1 ACVP (green rectangle), 3 OBS (yellow ellipse), TSS (yellow dashed circles), 1 ABS (yellow rectangle), 1 PPT (pink circle) and 1 SRP (blue ellipse).

Equipment position:

The Resistant Wave Gauges were placed at:

ID	X (m)
WG0	7.67
WG1	26
WG2	28.55
WG3	30.54
WG4	41.6
WG5	44.6
WG6	47.58
WG7	53.98
WG8	57.49
WG9	59.57
WG10	62.6
WG12	26.99
WG13	6.34

The Pore Pressure Sensors were placed at:

	X (m)	Z (m)	ID
PPT0	45.6	1.9	237
PPT1	56.6	1.9	302
PPT2	47.6	1.9	307
PPT3	48.6	1.9	058
PPT4	49.6	1.9	065
PPT5	52.6	1.9	056
PPT6	51.6	1.9	235
PPT7	50.6	1.9	236
PPT8	On the mobile frame		059

where z is the distance from the concrete bottom flume.

All deployed PPT had a measuring range of 0-400 mb with the exception of PPT 3, 4, 5 and 8 (with IDs 058, 065, 056 and 059) that have a measuring range of 0-100 mb.

The ADV were placed at:

ADV	ID	X(m)	Bottom distance (m)	D/S	PC
ADV0	387	53.14	0.24	D_as_S	1
ADV1	374	56.66	0.29	D_as_S	1
ADV2	435		on mobile frame	S	2
ADV3	336		on mobile frame	D_as_S	2
ADV4	285		on mobile frame	D_as_S	2
ADV5	281		on mobile frame	D_as_S	2

Where D_as_S notation means that Downlookings ADV were placed horizontally. This has to be taken into account when considering the x, y and z recording. X is always the X positive direction of the flume, but all the other axis will depend on the orientation of the measurement equipment. This has been considered and corrected for the binary .mat files but not in the raw .vno adv files.

The bottom distance of the ADV refers to the distance of the ADV above the sand bed. Considering the fact that both fixed frames were located in the flat part of the profile (located at 1.35 m above the flume floor), the distance of both ADV towards the concrete bottom is 1.59 and 1.64 m for ADV 0 and 1 respectively.

The relative location of the four ADV's on the mobile frame is ADV2, ADV3, ADV5 and ADV6 when going from the lower position (closer to the bottom) up the higher position respectively (see Figure 17, where the general sketch of all equipment on the mobile frame is presented).

Three Optical Backscatter Sensors were located on the mobile frame.

ADV	ID	Position within the frame
OBS0	T8267	lower (closer to the bottom)
OBS1	T8276	upper
OBS2	T8285	middle

Fixed frame (FF) ACVP's:

ACVP-FF	X(m)	Z(m) (w.r.t to ADV at fixed frame)
Dev 1	56.56	-0.292 (w.r.t. ADV 1) -0.086 (from 17/01/2014) +0.24 (from 21/01/2014)
Dev 3	53.01	-0.242 (w.r.t. ADV 0)

Remarks:

- * Z position of ACVP's to flume bottom was not measured. The distance of ACVP to the bed can be derived from the measurements themselves.
- * During test experiments (before 29 nov), position of ACVP-dev3 was -.262 m w.r.t. ADV 0.
- * Dev 1 and Dev 3 were buried during RB 1
- * During RB 2, Dev3 was removed. Hence, for this series the terms 'dev1' and 'dev3' refer to different settings of the same ACVP head (static resp. dynamic gain mode).
- * During RB 2, the fixed-frame ACVP was repositioned vertically twice: first time after run 64 (on 17/01/2014) with 20.6 cm upwards, second time after run 71 (21/01/2014) with 11 cm upwards.

Fixed positions of the CCM tanks

CCM	X(m)	Z(m) (w.r.t. floor; reference is top of CCM tank)
Tank 1	56.56	1.098
Tank 2	53.00	1.092

The height of the CCM probes was ~ 10 cm below the initial bed for all runs. During RB1 and RB2, the bed grew out of range, resulting in no data.

Changes done to the fixed frame measuring equipment during the different experimental days.

26/11/2013

The PPT are relocated to:

	X (m)	Z (m)	ID
PPT0	54.14	1.9	237
PPT1	55.35	1.9	302
PPT2	56.6	1.9	307
PPT3	58.55	1.9	058
PPT4	49.02	1.9	065
PPT5	53.00	1.9	056
PPT6	52.02	1.9	235
PPT7	50.52	1.9	236

10/12/2013

The PPT are relocated to:

	X (m)	Z (m)	ID
PPT3	58.55	2.19	058
PPT4	49.02	2.22	065
PPT5	52.95	2.22	056

21/01/2014

Changes done on the mobile frame (OBS T8276 and OBS T8267), suction nozzles, PPT 8 and Vectrino 2 included in Table 3.

Mobile frame	instrument	reference point	frame coordinates			
			x (mm)	y (mm)	Z _{bar} (mm)	Z _{floor} (mm)
mini frame	Vectrino II	centre transmitter	0	237	193	563
		centre trans from 13/12/2013	0	237	209,5	579,5
		centre trans from 21/01/2014	0	237	226,5	596,5
	ACVP	centre transmitter	-7,5	81	252	622
		centre trans from 13/12/2013	-7,5	81	242,5	612,5
		centre trans from 21/01/2014	-7,5	81	253,5	623,5
	OBS_1 (T8267)	centre transducer	-7,5	-73	196	566
		centre trans from 21/01/2014	-7,5	-73	235,5	605,5
	Nozzle_1	centre nozzle	-12,5	-295	154	524
		centre nozzle from 21/01/2014	-12,5	-295	280	650
	Nozzle_2	centre nozzle	2,5	-295	178	548
		centre nozzle from 21/01/2014	2,5	-295	254	624
	Nozzle_3	centre nozzle	25,5	-295	228	598
		centre nozzle from 21/01/2014	25,5	-295	227	597
	Nozzle_4	centre nozzle	46,5	-295	311	681
	Nozzle_5	centre nozzle	22,5	-295	439	809
main frame	Nozzle_6	centre nozzle	50	-200		1082
	Nozzle_7	centre nozzle	47	-200		1482
	ABS_1Mhz	centre transducer	-88	-432		1318
	ABS_2Mhz	centre transducer	-34	-432		1318
	ABS_3Mhz	centre transducer	33	-432		1315
	ABS_4Mhz	centre transducer	95	-432		1316
	ADV_0 (0435)	centre transmitter	-118	489		658
	ADV_1 (0336)	centre transmitter	16	597	502	872
	ADV_2 (0285)	centre transmitter	148	871		1315
	ADV_3 (0281)	centre transmitter	-65	868		1811
	Pressure tr.	centre head	-9	170	939	1309
		centre head from 21/01/2014	-9	0	278	1073
	OBS_2 (T8285)	centre transducer	-34	471		1310

OBS_3 (T8276)	centre transducer	59	490	1788
	centre trans from 21/01/2014	59	490	2046
SRP	centre transducer	638	633	1304
-	office sidewall	0	-1240	-
-	windowed sidewall	0	1754	-
-	other vert bar on frame	0	463	-

Table 3. Instrument measurement within the mobile frame.

frame coordinate system

$x = 0$ -> front (wave paddle side) of the main frame at the surface of the of the vertical bars (+ve towards beach)

$y = 0$ centre of the vertical bar at which the miniframe is attached (-ve to office side, +ve to window side)

$z_{bar} = 0$ (distance to horizontally levelled bar aligned in x-direction with miniframe)

$z_{floor} = 0$ (bottom of the flume)

flume coordinate system

$X_{tape} =$ reading on measuring tape along flume. For the trolley the read location at end of paddle-sided bright yellow clamp

$X = 0$ wave paddle in rest position (7.41m from start of tape)

$Z = 0$ bottom of flume (same as z_{floor})

$Y = 0$ office sidewall

Remarks:

* ADV fixed frame z positions are relative to ACVP pressure head. For fixed frame 2, distance was 262 mm during test experiments (runs before 29 nov)

Test programme

The profile shows that the profiler was run after the experiment to which it is linked. There is always an initial profile (P0) that is done before the start of the experiments.

Test	test/run	Waves	MWL	Filename	x // z frame	Profile	TSS	Aquascatt	Remarks
						P0			
22	test_029	H 0.6, T 3.5	2.5	261113_0	54.89 // 1.524			20131126104814	trigger for ADV failed,
23	test_030	H 0.85, T 4	2.5	261113_1	54.89 // 1.524		YES	20131126111932	pc1_ADV (delay of s)
24	test_031	H 0.85, T 4	2.5	261113_2	54.89 // 1.524		YES	20131126125537	pc1_ADV (delay of s). ABS 1 MHz on, ACVP_MF off
25	test_032	H 0.85, T 4	2.5	261113_3	55.87 // 1.479		YES	20131126161107	.lvm trigger failed (delay of s)
26	test_033	H 0.85, T 4	2.5	261113_4	55.87 // 1.437		YES	off	SRP scanner On
27	test_034	H 0.75, T 4.4	2.5	261113_5	55.87 // 1.417			off	SRP scanner on, ABS off
28	test_035	H 0.6, T 4.4	2.5	261113_6	55.87 // 1.417			off	SRP scanner on, ABS off
29	test_036	H 0.6, T 4.4	2.65	271113_0	55.47 // 1.540			off	SRP scanner on, ABS off
30	test_037	H 0.8, T 4.4	2.65	271113_1	55.47 // 1.540		YES	off	SRP scanner on, ABS off
31	test_038	H 0.68, T 5	2.65	271113_2	55.47 // 1.540	P8		off	SRP scanner on, ABS off
32		H 0.6, T 4.6	2.55	021213_1	55.50 // 1.531			off	pc2_ADV off
33	run_001	H 0.85, T 4	2.55	021213_2	55.50 // 1.531	P9	YES	20131202130602	.lvm (delay of 1' 50"). V2 stopped (9 min) and was restarted. ACVP_MF stopped as well.
34	run_002	H 0.85, T 4	2.55	021213_3	54.49 // 1.568	P10	YES	20131202150147	No records of OBS's and PPT on mobile frame.
35	run_003	H 0.85, T 4	2.55	021213_4	55.50 // 1.580	P11	YES	20131202160342	.lvm (delay of 6' 20") V2 stop at 9 min.
36	run_004	H 0.85, T 4	2.55	021213_5	54.50 // 1.550		YES	20131202170348	ADV3 off. V2 and ACVP_FF delay (s)
37		H 0.6, T 3.5	2.55	031213_0	57.85 // 1.550	P12			
38	run_005	H 0.85, T 4	2.55	031213_1	57.85 // 1.550		YES	20131203100827	V2 delay (s), stopped after 9 min
39	run_006	H 0.85, T 4	2.55	031213_2	51.00 // 1.550	P13		20131203105801	
40	run_007	H 0.85, T 4	2.55	031213_3	54.49 // 1.689			20131203121028	ABS emerged at through
41	run_008	H 0.85, T 4	2.55	031213_4	60.17 // 1.427	P14	YES	20131203124852	ABS (delay of 1'). ACVP_MF delay (s)
42	run_009	H 0.85, T 4	2.55	031213_5	55.51 // 1.708			20131203143607	ADV3 off; ABS emerged at through. V2 at 9 min stop.
43	run_010	H 0.85, T 4	2.55	031213_6	63.15 // 1.472	P15	YES	20131203150756	ADV3 off
44		H 0.85, T 4	2.55	041213_0	52.95 // 1.701				

45	run_011	H 0.85, T 4	2.55	041213_1	52.95 // 1.701			20131204100314	.lvm off; ABS (delay of 1' 40"); pc2_ADV cancelled after 20 ". V2 stop at 9 min. ABS sensors 3 and 4 MHz swapped (prob. Useless)
46	run_012	H 0.85, T 4	2.55	041213_3	56.42 // 1.616	P16	YES	20131204104140	ABS sensors 3 and 4 MHz swapped (prob. Useless)
47	run_013	H 0.85, T 4	2.55	041213_4	57.85 // 1.419			20131204113842	V2 stop at 9 min.
48	run_014	H 0.85, T 4	2.55	041213_5	51.02 // 1.562		YES	20131204122750	ABS emerged at through; ABS 4 probes measuring; ADV3 off, ACVP_MF off.
49	run_015	H 0.85, T 4	2.55	041213_6	51.02 // 1.562	P17		20131204125436	ADV3 off; Ripple scanner along the flume V2 crash 10.30 min.
50	run_016	H 0.85, T 4	2.55	041213_7	60.17 // 1.399		YES	20131204161121	ADV3 off; ABS 4 probes measuring
51	run_017	H 0.85, T 4	2.55	041213_8	60.17 // 1.387				.lvm off; ADV3 off; pc2_ADV off V2 crash 9 min.
52		H 0.85, T 4	2.55	051213_0	52.94 // 1.769				pc1_ADV (delay of m)
53	run_018	H 0.85, T 4	2.55	051213_1	52.94 // 1.769	P18	YES	20131205102953	ABS emerged at through
54	run_019	H 0.85, T 4	2.55	051213_2	57.84 // 1.324				.lvm off; ADV3 off. V2 crash 9 min.
55	run_020	H 0.85, T 4	2.55	051213_3	57.12 // 1.656		YES	20131205125108	ADV3 off V2 crash 9 min.
56	run_021	H 0.85, T 4	2.55	051213_4	58.49 // 1.318				ADV3 off; Ripple scanner continuously
57	run_022	H 0.85, T 4	2.55	051213_5	57.84 // 1.305	P19	YES		ADV3 off; Ripple scanner behind the bar
58	test_043	IGB1_4450	2.65	101213_1	58.27 // 1.480				
59	test_044	IGB1_4460	2.65	101213_2	58.27 // 1.480				
60	test_045	IGB1_4469	2.65	101213_3	58.27 // 1.480				
61	test_046	IGB1_5044	2.65	101213_4	58.27 // 1.480				
62	test_047	IGB1_5050	2.65	101213_5	58.27 // 1.480				
63	test_048	IGB1_5058	2.65	101213_6	58.27 // 1.480				
64	test_049	IGM1_4457	2.65	101213_7	58.27 // 1.480				
65	test_050	IGM2_4457	2.65	101213_8	58.27 // 1.480				
66	test_051	IGB1_5065	2.65	101213_9	58.27 // 1.480				
67	test_052	IGB1_4460	2.65	101213_10	58.27 // 1.480				
68	test_053	IGB1_4460	2.65	111213_0	58.27 // 1.480				
69	test_054	IGB1_4460	2.65	111213_1	58.27 // 1.480				
70	test_055	IGB1_4460	2.65	111213_2	58.27 // 1.480				.lvm off
71	test_056	IGB3_4455	2.65	111213_3	58.27 // 1.480				
72	test_057	IGB1_4460	2.65	111213_4	56.57 // 1.505				
73	test_058	IGB1_4460	2.65	111213_5	56.57 // 1.505				

74	test_059	IGB1_4460	2.65	111213_6	56.57 // 1.505				pc1 and pc2_ADV are stop at mid run to see interferences at ACVP
75	test_060	IGB1_4460	2.65	111213_7	56.57 // 1.505	P20			
76	run_023	IGB1_4460	2.65	121213_0	56.56 // 1.474	P22			P21 is measured before starting this case
77	run_024	IGB1_4460	2.65	121213_1	56.56 // 1.501		YES	20131212152405	V2 started before trigger (few seconds)
78	run_025	IGB1_4460	2.65	121213_2	56.56 // 1.501	P23			V2 started possibly before trigger (~second)
79	run_026	IGB1_4460	2.65	121213_3	56.56 // 1.487		YES	20131212172040	ABS delay of 30 "; ADV3 off; time series over after 1589 s
80	run_027	IGB1_4460	2.65	121213_4	56.56 // 1.487			20131212175245	ABS delay of 20"; ADV3 off
81	run_028	H 0.6, T 4	2.65	121213_5	56.56 // 1.487	P24			PPT off; ADV3 off
82	run_029	IGB1_4454	2.65	131213_0	58.51 // 1.483	P26			P25 is measured before starting this case; pc2_ADV (delay s); Ripple scanner continuously. V2 started before trigger (few seconds)
83	run_030	IGB1_4454	2.65	131213_1	58.51 // 1.487		YES	20131213130954	ADV3 off V2 started before trigger (few seconds)
84	run_031	IGB1_4454	2.65	131213_2	58.51 // 1.487	P27			pc1_ADV off; ADV3 off; Ripple scanner continuously V2 started before trigger (~1second)
85	run_032	IGB1_4454	2.65	131213_3	58.51 // 1.487				ADV3 off; Ripple scanner continuously
86	run_033	IGB1_4454	2.65	131213_4	58.51 // 1.487	P28	YES	20131213160815	pc2_ADV (delay 3"); ADV3 off
87	run_034	IGM1_4463	2.65	161213_0	58.51 // 1.496	P30			P29 is measured before starting this case
88	run_035	IGM1_4463	2.65	161213_1	58.51 // 1.499		YES	20131216125640	ADV3 off
89	run_036	IGM1_4463	2.65	161213_2	58.51 // 1.504	P31			ADV3 off
90	run_037	IGM1_4463	2.65	161213_3	58.51 // 1.499				ADV3 off. SRP on
91	run_038	IGM1_4463	2.65	161213_4	58.51 // 1.491	P32	YES	20131216164452	ADV3 off. V2 stopped during acq. ABS 1 MHz on.
92	run_039	IGM2_4463	2.65	171213_0	58.52 // 1.508	P34			P33 is measured before starting this case
93	run_040	IGM2_4463	2.65	171213_1	58.51 // 1.517		YES	20131217123041	ADV3 off
94	run_041	IGM2_4463	2.65	171213_2	58.51 // 1.487	P35			ADV3 off
95	run_042	IGM2_4463	2.65	171213_3	58.51 // 1.509				ADV3 off
96	run_043	IGM2_4463	2.65	171213_4	58.51 // 1.509	P36	YES	20131217161605	ADV3 off
97	run_044	H 0.44, T 4.4	2.65	181213_0	58.51 // 1.514	P38			P37 is measured before starting this case
98	run_045	H 0.44, T 4.4	2.65	181213_1	58.51 // 1.507			20131218132648	
99	run_046	H 0.44, T 4.4	2.65	181213_2	58.51 // 1.528	P39	YES	20131218135600	ACVP_MF last few waves missed.
100	run_047	H 0.61, T 4.4	2.65	181213_3	58.51 // 1.519	P40			
101	run_048	H 0.61, T 4.4	2.65	181213_4	58.51 // 1.543			20131218161959	ADV3 off
102	run_049	H 0.61, T 4.4	2.65	181213_5	58.51 // 1.509	P41	YES	20131218165024	ADV3 off. V2 delay (s)

103	run_050	H 0.69, T 4.4	2.65	181213_6	58.51 // 1.520			20131218174559	ADV3 off
104	run_051	H 0.69, T 4.4	2.65	181213_7	58.51 // 1.547	P42	YES	20131218181414	ADV3 off
105	run_052	IGB2_4460	2.65	191213_0	58.51 // 1.536	P44			P43 is measured before starting this case
106	run_053	IGB2_4460	2.65	191213_1	58.51 // 1.544		YES	20131219132214	
107	run_054	IGB2_4460	2.65	191213_2	58.51 // 1.544	P45		20131219135849	pc1_ADV started 4-5' before. Both SRP and ABS on.
108	run_055	IGB2_4460	2.65	191213_3	58.51 // 1.529			20131219154059	ADV3 off. Both SRP and ABS on
109	run_056	IGB2_4460	2.65	191213_4	58.51 // 1.523	P46	YES	20131219161723	ADV3 off. V2 delay (s). ACVP_MF only recorded last part.
110	test_061	IGB_4086	2.65	191213_5	54.78 // 1.516	P47			ADV3 off
111	test_062	H 0.6, T 4	2.65	160114_0	55.50 // 1.508				P48 is measured before starting this case
112	test_063	H 0.95, T 4	2.65	160114_1	55.50 // 1.508				pc2_ADV failed
113	test_064	H 0.78, T 4.5	2.65	160114_2	55.50 // 1.508				
114	test_065	H 0.85, T 3.5	2.65	160114_3	55.50 // 1.508				
115	test_066	H 0.9, T 3.5	2.65	160114_4	55.50 // 1.508	P49			
116	run_057	H 0.95, T 4	2.65	160114_5	55.50 // 1.503			20140116110837	
117	run_058	H 0.95, T 4	2.65	160114_6	57.85 // 1.577	P50		20140116114839	
118	run_059	H 0.95, T 4	2.65	160114_7	54.51 // 1.567			20140116124046	ADV3 off. V2 delay (m), launched on 3 rd CCM trigger.
119	run_060	H 0.95, T 4	2.65	160114_8	56.42 // 1.542	P51		20140116131619	ADV3 off
120	run_061	H 0.95, T 4	2.65	160114_9	59.18 // 1.591			20140116151419	ADV3 off. ACVP_MF delay (s)
121	run_062	H 0.95, T 4	2.65	160114_10	52.95 // 1.538	P52		20140116155104	ADV3 off; Echosounders may not be perpendicular to the wall
122	run_063	H 0.95, T 4	2.65	160114_11	60.70 // 1.570			20140116164020	ADV3 off
123	run_064	H 0.95, T 4	2.65	160114_12	55.50 // 1.634	P53		20140116171315	ADV3 off; Echosounders may not be perpendicular to the wall
124		H 0.95, T 4	2.65	200114_0	56.42 // 1.669				
125	run_065	H 0.95, T 4	2.65	200114_1	56.42 // 1.669			20140120100244	25 ' time series
126	run_066	H 0.95, T 4	2.65	200114_2	59.18 // 1.611	P54		20140120104215	ACVP_MF delay (m), dev3 was lost.
127	run_067	H 0.95, T 4	2.65	200114_3	57.85 // 1.725				30 ' time series; ADV3 off
128	run_068	H 0.95, T 4	2.65	200114_4	54.51 // 1.662			20140120123611	pc1_ADV (delay 3 m); ADV3 off. V2 delay (s) (3 rd trigger)
129		H 0.95, T 4	2.65	200114_5	55.50 // 1.715				ADV3 off; time series stops after a few seconds due to a measuring problem
130	run_069	H 0.95, T 4	2.65	200114_6	55.50 // 1.715	P55		20140120132304	ADV3 off
131	run_070	H 0.95, T 4	2.65	200114_7	56.42 // 1.791			20140120151233	ADV3 off; ABS and PPT emerged at the wave trough. V2 data incomplete

132	run_071	H 0.95, T 4	2.65	200114_8	57.85 // 1.902	P56		20140120162215	ADV3 off. V2 delay (~2 m).
133		H 0.95, T 4	2.65	210114_0	59.18 // 1.921				pc1_ADV (delay)
134	run_072	H 0.95, T 4	2.65	210114_1	59.18 // 1.921			20140121143410	
135	run_073	H 0.95, T 4	2.65	210114_2	60.70 // 1.713	P57		20140121151349	ABS (dealy m)
136	run_074	H 0.95, T 4	2.65	210114_3	62.77 // 1.451	P58		20140121163133	ADV3 off; ABS (delay m)
137		H 0.95, T 4	2.65	220114_0	60.70 // 1.613				ADV3 off
138	run_075	H 0.95, T 4	2.65	220114_1	60.70 // 1.613	P59		20140122103234	ADV3 off. ABS 1 MHz on, ACVP_MF off.
139	run_076	H 0.95, T 4	2.65	220114_2	60.70 // 1.559	P60		20140122115223	ADV3 off, SRP continuous run but stopped (bubbles)
140	run_077	H 0.95, T 4	2.65	220114_3	52.95 // 1.527			20140122130315	ADV3 off
141	run_078	H 0.95, T 4	2.65	220114_4	52.95 // 1.527	P61		20140122141822	ADV3 off. ABS 1 MHz on, ACVP_MF off
142	run_079	H 0.95, T 4	2.65	220114_5	54.51 // 1.608			20140122155912	ADV3 off
143	run_080	H 0.95, T 4	2.65	220114_6	54.51 // 1.633	P63		20140122163236	ADV3 off ABS 1 MHz on, ACVP_MF off
144	run_081	H 0.95, T 4	2.65	220114_7	51.42 // 1.402			20140122175622	ADV3 off
145		H 0.95, T 4	2.65	230114_0	51.42 // 1.383				pc2_ADV (delay m)
146	run_082	H 0.95, T 4	2.65	230114_1	51.42 // 1.383	P65		20140123105702	ABS 1 MHz on, ACVP_MF off

Table 4. Test Programme

Notes on the experimental tests:

x frame refers to the position of the mobile frame relative to the wave paddle. = 7.41 (distance from the wave paddle to the tape 0) + position of the trolley beginning at the tape - 0.711 (distance of the frame relative to the beginning of the trolley where the tape reading is taken)

z frame is the absolute reference of the ADV0 (435) to the concrete bottom of the flume = reading on the frame display + 0.658 which is the distance of the ADV0 towards the bottom.

Aquascatt off // Rip scanner On: This means that during this case the Aquascatt was turn off and the Ripple Scanner measured continuously during this entire case.

delay of s: The measuring equipment did not work properly and there is some delay of several seconds.

delay of m: The measuring equipment did not work properly and there is some delay of several minutes.

.lvm refers to the external files acquired with the external National instrument DAQ. This computer controls the PPT and 3 OBS on the movable frame.

The Vectrino Profiler (V2) experienced 2 sorts of problems: (1) did often not start properly on trigger; (2) stopped acquisition after 9 min 11 seconds.

5 Organization of data files

The data files are organized following the next scheme:

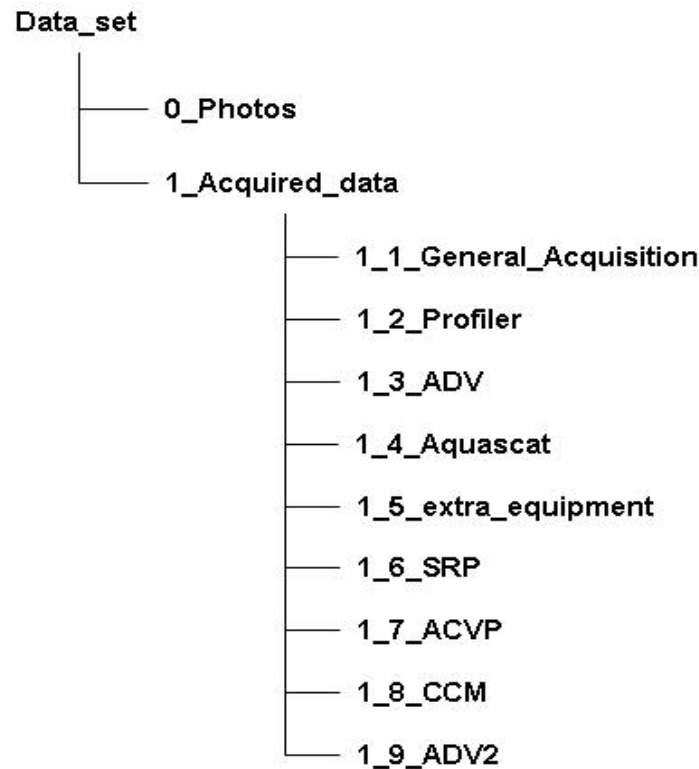


Figure 18. File organization scheme of all acquired data .

In Table4, the filename of each experiment can be found and correlated with the data storage information. The filename can be found with a .txt extension for the general acquisition data and a .vno extension for the ADV acquisition data. There are mainly three groups of files.

1. .txt files are in 1_1_General_Acquisition. These files contain the information acquired directly by the general acquisition system of the wave paddle, which controls the absolute time reference, resistive and acoustic wave gauges signals, OBS, Pressure Sensors and synchronization signals of other equipment. The format of these files is as follows: five initial rows in which the frequency of the acquisition can be seen in the second row, and the acquisition channel name and measuring units can be read in the sixth row. The information of each probe is found consecutively in time considering the acquisition frequency used at the experiment.
2. Profile information is stored in individual files PX.txt containing the information provided by the bed profiler of all the performed runs (X representing the profile number), found in 1_2_Profiler section. Each profile is structured in three columns. The first column is for the X cross-shore location along the flume (where X = 0 is the position of the wave paddle at resting position). The second and third column (echo1 and echo2 respectively) report the information of both echosounders at each X position. The depth of the echosounders is relative to the bed location. It has to be adjusted using the maximum water depth or the initial fixed part of the profile. The approximate time at which each profile measurement has been done can be found in the test programme section of this document.
3. .vno files are found in 1_3_ADV. This second group is formed by the ADV information acquired by means of the Polysink Software. These files can be extracted directly with the aid of this software (providing velocities, correlation, signal amplitude, signal to noise

- ratio, temperature and control files) or can be converted by the “Nortek file converter” and analyzed using the WinADV software freely available on the net. (free version of both programs can be found at www.nortek-as.com).
4. .aqa files are in 1_4_Aquascap. These files contain the information gathered by the Aquascap measurement equipment. The data can be visualized and later on post processed by means of AQUAview1000 software from the Aquatecgroup corporation (www.aquatecgroup.com). Alternatively, Aquatec have supplied a Matlab based conversion script which is better for converting large numbers of files (note that Richard Cooke at NOC Liverpool has written an adjusted version RDCO_Aquascap_MatLab_processor.m).
 5. .lvm files are in 1_5_Extra_equipment. These files contain the information obtained with a National Instrument acquisition module that was on the mobile trolley. This module measured at a sampling frequency of 100 Hz the information of the 3 OBS and 1 PPT that were not linked to the General acquisition system. The trigger of this acquisition system was on the rising edge of the trigger signal and therefore it is starting to measure at the same time as the ADV's and General Acquisition system. The files are simply txt ascii files that contain 4 columns that correspond to: OBS T8267, OBS T8285, OBS T8276 and PPT 059 respectively.
 6. SRP, The raw SRP backscatter data are stored in comma-separated ASCII files which will be accepted by most data analysis programs and spreadsheets. The first 6 lines of each ASCII file contains the SRP settings, the remainder contains the digitized backscatter data, where for each row the angle is the first parameter and the remainder contains the 8-bit digitized backscatter data for the 1000 data bins. Note that the unit of the angle is Gradians where 200 is the centre of each swath.
The processed data is stored in space-delimited ASCII files whereby the filename is structured as follows run### #####.rip, e.g. run001 735570.rip. The first three digits indicate the run number and the six digit number following the underscore is the serial data number, which can be converted into a string using the MATLAB function datestr, e.g. datestr(735570) gives 02-Dec-2013. The first cell of the file contains the 6-digit serial date number and the remainder of the first row contains the cross-shore coordinate in meters. Each consecutive row contains the measured bed elevations in m distance from the transducer head, with the first cell containing the serial date and time-stamp of the bed measurement. Below is given an example of how to load the data from a *.rip file in MATLAB.


```
data=dlmread(run001 735570.rip,',' )
X=data(1,2:end);
t=datevec(data(2:end,1));
z=data(2:end,2:end);
```
 7. ACVP: .raw ascii ACVP files, can be translated to separate ascii files for velocity components u and w, intensity of the signals, correlation, and intensity of bed. ACVP files are provided on request.
 8. CCM: .lvm file, ascii format. Columns with time, concentration measurements of 4 probes, positions of 3 probes, input trigger, output trigger, and optional analogue input from additional instruments, sampled through the CCM acquisition system. The CCM data files are provided on request
 9. ADV 2: have already been translated to *.mat files. These *.mat files include metadata, stored in variable 'Config'. Main variables: time, u, v, w, correlation, intensity, SNR, bottom distance measurement. ADV 2 files are provided on request.

6 References

- Bosman, J. J., van der Velden, E. T., and Hulsbergen, C. H., 1987. Sediment concentration measurement by transverse suction. *Coastal Engineering*, 11(4):353–370.
- Butt, T., Miles, J., Ganderton, P., Russell, P., 2002. A simple method for calibrating optical backscatter sensors in high concentrations of non-cohesive sediments. *Marine Geology* 192 (4), 419–424.
- Chassagneux, F. X., and Hurther D., 2014. Wave bottom boundary layer processes below irregular surf zone breaking waves with light-weight sheet flow particle transport, *J. Geophys. Res. Oceans*, 119
- Doucette, J. S. and O'Donoghue, T., 2006. Response of sand ripples to change in oscillatory flow. *Sedimentology*, 53(0):581–596.
- Hurther, D., and Thorne, P. D., 2011. Suspension and near-bed load sediment transport processes above a migrating, sand-rippled bed under shoaling waves. *Journal of Geophysical Research C: Oceans*, 116.
- Hurther, D., Thorne, PD, Bricault M, Lemmin U and Baroud JM., 2011. A multi-frequency acoustic concentration and velocity profiler (ACVP) for boundary layer measurements of fine-scale flow and sediment transport processes. *Coastal Engineering*, Vol. 58: 594-605.
- Naqshband S, Ribberink, J. S, Hurther D. and Hulscher, S.J.M.H., 2014. Bed load and suspended load contributions to migrating sand dunes in equilibrium. *J. Geophys. Res. Earth Surface*, 119.
- O'Hara Murray, R. B., Thorne, P. D., and Hodgson, D. M., 2011. Intrawave observations of sediment entrainment processes above sand ripples under irregular waves. *J. Geophys. Res.*, 116(C1):C01001.
- Schretlen, J. L. M., 2012. Sand transport under full-scale progressive surface waves. PhD Thesis, University of Twente, The Netherlands.
- Thorne, P. D., Williams, J. J., and Davies, A. G., 2002. Suspended sediment under waves measured in a large scale flume facility. *J. Geophys. Res.*, 107(C8):4.1–4.16.
- Thorne, P. D., and Hurther, D., 2014. An overview on the use of backscattered sound for measuring suspended particle size and concentration profiles in non-cohesive inorganic sediment transport studies. *Continental Shelf Research*, Vol. 73: 97–118.